expression. We reconstituted the functional chemiluminescent protein by incubating the intact cells with 2.5 μM coelenterazine for 2 to 3 hours before an experiment (*8*); cells were also incubated with fura-2/AM for the last 30 min before an experiment (*11*). After reconstitution, the monolayer of HeLa cells, grown on a small glass cover slip (13 mm in diameter), was washed with fresh medium and introduced into the perfusion chamber; light emission was measured with a luminometer [P. H. Cobbold and J. A. C. Lee in *Cellular Calcium, A Practical Approach*, J. G. McCormack and P. H. Cobbold, Eds. (IRL Press, Oxford, 1991), pp. 55–81]. The perfusion chamber was maintained at 37°C by a water jacket. To obtain a rapid and synchronous equilibration of medium in the chamber, during the changes of medium the flow rate was increased from 2.5 to 6 ml/min. The time necessary for the new medium to reach the perfusion chamber was 12 ± 1 s ($n = 5$), and 50% equilibration was obtained in 2 s. The light emission from aequorin was transformed into $[Ca^{2+}]_m$ by means of a program provided by R. Cuthbertson, assuming an intramitochondrial Mg^{2+} concentration of 1 mM [G. A. Rutter, N. J. Osbaldeston, J. G. McCormack, R. M. Denton, *Biochem. J.* **271**, 627 (1990)]. In each experiment we obtained the final discharge of unconsumed aequorin, necessary for calibration, by exposing the cells to a solution of 10 mM $CaCl_2$.

10. M. D. Bootman, M. J. Berridge, C. W. Taylor, *J. Physiol.* **450**, 163 (1992).
11. Fura-2 loading was done as described [A. Malgaroli, D. Milani, J. Meldolesi, T. Pozzan, *J. Cell Biol.* **105**, 2145 (1988)]. Two types of cover slips were used. One, 20 mm long and 8 mm wide, was held in place in the cuvette of a multiwavelength fluorimeter maintained at 37°C (Cairn Research Ltd., Sittingbourne, Kent, UK, excitation at 350 and 380 nm, emission at 500 nm), as described [F. Di Virgilio, B. C. Meyer, S. Greenberg, S. C. Silverstein, *J. Cell Biol.* **106**, 657 (1988)]. In this type of experiment the signal represents the average of a few thousand cells illuminated by the incident beam. At the end of each experiment, ionomycin (2 μM) and then Mn^{2+} (1 mM) were added to obtain the background signal to be subtracted before calculating $[Ca^{2+}]_i$. The second type of cover slip, diameter 24 mm, was placed in a chamber held at 37°C with a thermostat (Medical System Corporation, Greenvale, NY) on the stage of an inverted fluorescent microscope (Zeiss Axiovert 100TV) equipped with the imaging apparatus (Analytical Imaging Concepts, Atlanta, GA) for fura-2 measurement. The $[Ca^{2+}]_i$ images (1 image per second) were calculated off-line after subtraction of the background (obtained as above) from each single image. The absolute values of $[Ca^{2+}]_i$ were calculated as described [G. Grynkiewicz, M. Poenie, R. Y. Tsien, *J. Biol. Chem.* **260**, 3440 (1985); A. Malgaroli, D. Milani, J. Meldolesi, T. Pozzan, *J. Cell Biol.* **105**, 2145 (1988)].
12. R. Rizzuto *et al.*, in preparation; R. Rizzuto, P. Bernardi, M. Favaron, G. F. Azzone, *Biochem. J.* **246**, 271 (1987).
13. Permeabilization with digitonin, a detergent preferentially directed toward membranes containing cholesterol, has been used to study the function of mitochondria in situ. Digitonin treatment of HeLa or endothelial cells results in complete release of the cytosolic marker enzyme lactic dehydrogenase, whereas the mitochondrial marker enzymes citrate synthase or glutamate dehydrogenase and recombinant chimeric aequorin remain associated with sedimented cells.
14. Similar values of $[Ca^{2+}]_i$ are measured with fura-2 and with injected aequorin in hepatocytes [N. M. Woods, K. S. R. Cuthbertson, P. H. Cobbold, *Nature* **319**, 600 (1986); T. A. Rooney, E. J. Sass, A. P. Thomas, *J. Biol. Chem.* **264**, 17131 (1989)]. In cells transfected with cytosolic aequorin, the peak $[Ca^{2+}]_i$ measured with this method closely agrees with that measured with fura-2 (R. Rizzuto *et al.*, unpublished data).
15. The concentration of Ca^{2+} in the buffers was calculated as described [A. Fabiato, in *Cellular Calcium, A Practical Approach*, J. G. McCormack and P. H. Cobbold, Eds. (IRL Press, Oxford, 1991), pp. 159–176]. The calculated concentrations of free Ca^{2+} in the medium were always compared with the values measured directly with fura-2 in an aliquot of the same buffers. If a discrepancy was noticed, the values measured with fura-2 were considered correct.
16. A discrepancy between the increases in $[Ca^{2+}]_i$ in intact cells measured with fura-2 and the calculated extramitochondrial $[Ca^{2+}]$ is observed also in the case of Ca^{2+} influx. The difference (approximately a factor of 2) may be ascribed to the loss of a cytosolic factor, perhaps spermine [J. G. McCormack, H. M. Brown, N. J. Dawes, *Biochim. Biophys. Acta* **973**, 420 (1989)].
17. R. Rizzuto *et al.*, unpublished data.
18. T. Satoh *et al.*, *J. Cell Biol.* **111**, 615 (1990); K. Takei *et al.*, *J. Neurosci.* **12**, 489 (1992).
19. If, after permeabilization, ATP was omitted, the response to IP_3 was reduced and eventually disappeared. Marginal increases of $[Ca^{2+}]_m$ were observed if the uncoupler of mitochondrial respiration *p*-(trifluoro-methoxy)phenylhydrazone (FCCP) was included in the buffer before the addition of IP_3. Substitution of EGTA with an equivalent concentration of the faster Ca^{2+} chelator BAPTA did not change the effect of IP_3 on $[Ca^{2+}]_m$. Conversely, when high concentrations of either chelator were used (for example, 500 μM), the IP_3-induced $[Ca^{2+}]_m$ transient was virtually abolished.
20. J. E. Chad and R. Eckert, *Biophys. J.* **45**, 993 (1984); S. M. Simon and R. Llinás, *ibid.* **48**, 485 (1985); G. J. Augustine and E. Neher, *Curr. Opin. Neurobiol.* **2**, 302 (1992).
21. R. Llinás, M. Sugimori, R. B. Silver, *Science* **256**, 677 (1992).
22. A. J. O'Sullivan *et al.*, *EMBO J.* **8**, 401 (1989); T. A. Rooney, E. J. Sass, A. P. Thomas, *J. Biol. Chem.* **265**, 10792 (1990).
23. Supported by grants from the Italian Research Council (CNR) "Biotechnology" and "Oncology," from "Telethon," from the Italian Association for Cancer Research (AIRC), and from the "AIDS Project" of the Italian Health Ministry to T.P. We thank Y. Kishi for the gift of coelenterazine; Y. Sakaki for the aequorin cDNA; P. H. Cobbold and R. Cuthbertson for the data analysis software and for advice on the construction of the aequorin detection system; G. Ronconi and M. Santato for technical assistance; C. Bastianutto and L. Pasti for carrying out some of the experiments; J. Meldolesi, C. Montecucco, G. Schiavo, and P. Volpe for critically reading the manuscript; R. Bruzzone for discussion; and G. F. Azzone for encouragement and support.

14 May 1993; accepted 30 August 1993

Alterations of a Zinc Finger–Encoding Gene, *BCL-6*, in Diffuse Large-Cell Lymphoma

Bihui H. Ye, Florigio Lista,* Francesco Lo Coco,† Daniel M. Knowles, Kenneth Offit, R. S. K. Chaganti, Riccardo Dalla-Favera‡

The molecular pathogenesis of diffuse large-cell lymphoma (DLCL), the most frequent and clinically relevant type of lymphoma, is unknown. A gene was cloned from chromosomal translocations affecting band 3q27, which are common in DLCL. This gene, *BCL-6*, codes for a 79-kilodalton protein that is homologous with zinc finger–transcription factors. In 33 percent (13 of 39) of DLCL samples, but not in other types of lymphoid malignancies, the *BCL-6* gene is truncated within its 5′ noncoding sequences, suggesting that its expression is deregulated. Thus, *BCL-6* may be a proto-oncogene specifically involved in the pathogenesis of DLCL.

The molecular analysis of specific chromosomal translocations has improved our understanding of the pathogenesis of non-Hodgkin lymphoma (NHL), a heterogeneous group of B cell and (less frequently) T cell malignancies (*1*, *2*). The (14;18) chromosomal translocation, which causes the deregulated expression of the anti-apoptosis gene *BCL-2*, plays a critical role in the development of follicular lymphoma (FL) (*3*), which accounts for 20 to 30% of all NHL diagnoses (*4*). Burkitt's lymphoma (BL) and mantle-cell lymphoma, two relatively rare NHL types, are characterized by chromosomal translocations that cause the deregulated expression of the cell-cycle progression genes *MYC* and *BCL-1*/cyclin D1, respectively (*5*, *6*).

Relatively little is known about the molecular pathogenesis of DLCL, the most frequent and most lethal human lymphoma (*4*). It accounts for ~40% of initial NHL diagnoses and is often the final stage of progression of FL (*4*). A small percentage of DLCLs display *MYC* rearrangements (*7*) and 20 to 30% display alterations of *BCL-2*, reflecting the tumor's derivation from FL (*8*). However, no consistent molecular alteration has been identified that is specific for DLCL.

B. H. Ye, F. Lista, F. Lo Coco, D. M. Knowles, R. Dalla-Favera, Department of Pathology, College of Physicians and Surgeons, Columbia University, New York, NY 10032.
K. Offit and R. S. K. Chaganti, Cell Biology and Genetics Program and the Department of Pathology, Memorial Sloan-Kettering Cancer Center, New York, NY 10021.

*Also at the Centro Studi e Ricerche della Sanita' dell' Esercito, Rome, Italy.
†Also at the Sezione di Ematologia, Dipartimento di Biopatologia Umana, Universita' La Sapienza, Rome, Italy.
‡To whom correspondence should be addressed.

Chromosomal translocations involving reciprocal recombinations between band 3q27 and several other chromosomal sites are found in 8 to 12% of NHL cases, particularly in DLCL (9). From NHL samples displaying recombinations between 3q27 and the immunoglobulin heavy chain (IgH) locus on 14q32, we and others have cloned the chromosomal junctions of several (3;14)(q27;q32) translocations and identified a cluster of breakpoints at a 3q27 locus named *BCL-6* (*10*). Genomic sequences flanking the cluster region are transcriptionally active, suggesting that they contain a gene potentially involved in DLCL pathogenesis (*10*). In this study, we identify the *BCL-6* gene and its predicted protein product. We also demonstrate that structural lesions of this gene are common in DLCL.

To isolate normal *BCL-6* complementary DNA (cDNA), we screened a cDNA library constructed from the NHL cell line Bjab (*11*) with a probe (*10*) derived from the chromosomal region flanking the breakpoints of two t(3;14)(q27;32) cases. Sequence analysis (Fig. 1) revealed that the longest clone (3549 bp), about the same size as *BCL-6* RNA, codes for a protein of 706 amino acids with a predicted molecular mass of 79 kD. The putative ATG initiation codon at position 328 is surrounded by a Kozak consensus sequence (*12*) and is preceded by three upstream in-frame stop codons. The 1101-bp 3′ untranslated region contains a polyadenylation signal followed by a track of polyadenylate. These features are consistent with the idea that *BCL-6* is a functional gene (see Fig. 1A for a schematic representation of the cDNA clone).

The NH_2- and COOH-termini of the *BCL-6* protein (Fig. 1) (*13*) have homologies with zinc finger–transcription factors (*14*). A gene sequence encoding a nearly identical protein was recently deposited in GenBank. This gene, termed *LAZ-3*, was cloned on the basis of its involvement in 3q27 translocations, and it is therefore likely that *BCL-6* and *LAZ-3* are the same gene (*15*). Because the COOH-terminal region of *BCL-6* contains six C_2H_2 zinc finger motifs (Fig. 1) and a conserved stretch of six amino acids (the His-Cys link) connecting the successive zinc finger repeats (*16*), *BCL-6* can be assigned to the Krüppel-like subfamily of zinc finger proteins. The NH_2-terminal region of *BCL-6* is devoid of the FAX (*17*) and KRAB (*18*) domains sometimes seen in Krüppel-related zinc finger proteins, but it does have homologies (Fig. 2) with other zinc finger–transcription factors including the human ZFPJS protein, a putative human transcription factor that regulates the major histocompatibility complex II promoter (*19*), the Tramtrack (ttk) and Broad-complex (Br-c) proteins in *Drosophila* that regulate developmental transcription (*20*), the human KUP protein (*21*), and the human PLZF protein, which is occasionally involved in chromosomal translocations in human promyelocytic leukemia (*22*). The regions of NH_2-terminal homology among ZFPJS, ttk, Br-c, PLZF, and *BCL-6* also share homology with viral proteins (for example, VA55R) of the poxvirus family (*23*) as well as with the *Drosophila* kelch protein involved in nurse cell–oocyte interaction (*24*). These structural homologies suggest that *BCL-6* may function as a DNA binding transcription factor that regulates organ development and tissue differentiation.

The cDNA clone was used as a probe to investigate *BCL-6* RNA expression in a variety of human cell lines by Northern (RNA) blot analysis. A single 3.8-kb RNA species was readily detected (Fig. 2) in cell lines derived from mature B cells, but not from pro–B cells or plasma cells, T cells, or other hematopoietic cell lineages (*25*). The *BCL-6* RNA was not detectable in other normal tissues, except for skeletal muscle, which expressed low amounts (*25*). Thus, the expression of *BCL-6* was detected in B cells at a differentiation stage corresponding to that of DLCL cells. This selective expression in a "window" of B cell differentiation suggests that *BCL-6* may play a role in the control of normal B cell differentiation and lymphoid organ development.

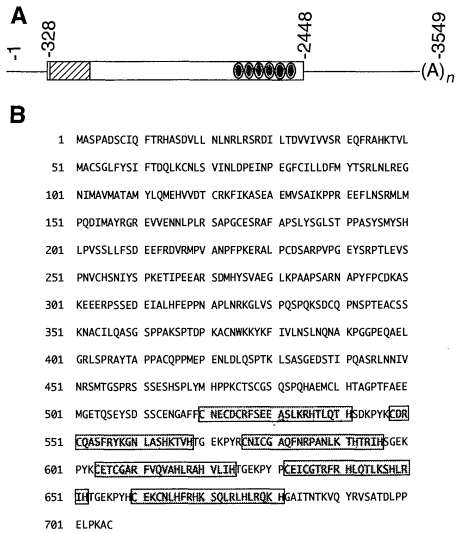

Fig. 1. Structure of *BCL-6* cDNA and sequence of its predicted protein product. (**A**) Schematic representation of the full-length *BCL-6* cDNA clone showing the relative position of the open reading frame (box) with 5′ and 3′ untranslated sequences (lines flanking the box). The approximate positions of the zinc finger motifs (shaded ovals) and the NH_2-terminal homology (striped area) with other proteins are also indicated. (**B**) The predicted amino acid sequence of the *BCL-6* protein. The residues corresponding to the six zinc finger motifs (shaded boxes) are shown. Note the repeated residues between the zinc finger motifs (His-Cys links). The GenBank accession number of *BCL-6* cDNA and amino acid sequences is U00115.

To characterize the *BCL-6* genomic locus, we used the same cDNA probe to screen a genomic library from human placenta (*26*). By restriction mapping, hybridization with various cDNA probes, and limited nucleotide sequencing, the *BCL-6* gene was found to contain at least eight exons spanning ~26 kb of DNA (Fig. 3). Sequence analysis of the first and second exons indicated that they are noncoding and that the translation initiation codon is within the third exon.

Various cDNA and genomic probes were used in Southern (DNA) blot hybridizations to determine the relation between 3q27 breakpoints and *BCL-6* sequences in a panel of 17 DLCL cases carrying chromosomal translocations involving 3q27 (Table 1). Monoallelic rearrangements of *BCL-6* were detected in 12 of 17 tumors with combinations of restriction enzymes (Bam HI and Xba I) and probes that explore ~16 kb of the *BCL-6* locus. These 12 positive cases carry recombinations between 3q27 and several different chromosomes (Table 1), indicating that heterogeneous 3q27 breakpoints cluster in a restricted genomic locus irrespective of the partner chromosome involved in the translocation. Some DLCL samples (5 of 17) do not display *BCL-6* rearrangements despite cytogenetic alterations in band 3q27, suggesting that another gene is involved or, more likely, that there are other breakpoint clusters 5′ or 3′ to *BCL-6*. If the latter is true, the observed frequency of *BCL-6* involvement in DLCL (33%) may be an underestimate.

We also analyzed a panel of tumors not previously selected on the basis of 3q27 breakpoints but representative of the major subtypes of NHL as well as of other lym-

Table 1. Frequency of *BCL-6* rearrangements in DLCL with chromosomal translocations affecting band 3q27.

Translocation	Fraction of tumors* with *BCL-6* rearrangements
t(3;14)(q27;q32)	4/4
t(3;22)(q27;q11)	2/3
t(3;12)(q27;q11)	1/1
t(3;11)(q27;q13)	1/1
t(3;9)(q27;q13)	0/1
t(3;12)(q27;q24)	0/1
der(3)t(3;5)(q27;q31)	1/1
t(1;3)(q21;q27)	1/1
t(2;3)(q23;q27)	1/1
der(3)t(3;?)(q27;?)	1/3

*Tumor samples were collected and analyzed for histopathology and cytogenetics at Memorial Sloan-Kettering Cancer Center.

phoproliferative diseases. Rearrangements of *BCL-6* were detected in 13 of 39 DLCLs, but not in other tumors including other NHL subtypes (28 FL, 20 BL, and 8 small lymphocytic NHL), acute lymphoblastic leukemia (ALL; 21 cases), and chronic lymphocytic leukemia (CLL; 31 cases). These findings indicate that *BCL-6* rearrangements are specific for and frequent in DLCL. In addition, the frequency of rearrangements in DLCL (33%) significantly exceeds that (8 to 12%) reported on the basis of cytogenetic studies (9), suggesting that some of the observed rearrangements may involve submicroscopic chromosomal alterations.

All the breakpoints in *BCL-6* mapped to the putative 5′ flanking region, the first exon, or the first intron (Fig. 3). For two patients that carry (3;14)(q27;q32) translocations, the chromosomal breakpoints have been cloned and precisely mapped to the first intron (SM1444) or to 5′ flanking sequences (KC1445) of *BCL-6* on 3q27 and to the switch region of IgH on 14q32 (*10*). In all rearrangements, the coding region of *BCL-6* was left intact, whereas the 5′ regulatory region, presumably containing the promoter sequences, was either completely removed or truncated. The resultant fusion of *BCL-6* coding sequences to heterologous (from other chromosomes) or alternative (within the *BCL-6* locus) regulatory sequences may disrupt the gene's normal expression pattern (*27*).

Zinc finger–encoding genes are plausible candidate oncogenes as they have been shown to participate in the control of cell proliferation, differentiation, and organ pattern formation (*14*). In fact, alterations of zinc finger genes have been detected in a variety of tumor types. These genes include *PLZF* (*22*) and *PML* in acute promyelocytic leukemia, *EVI-1* in mouse and human myeloid leukemia, *TTG-1* in T cell ALL, *HTRX* in acute mixed-lineage leukemia, and *WT-1* in Wilms tumor (*28*). Terminal differentiation of hematopoietic cells is associated with the down-regulation of many Krüppel-type zinc finger genes (*14, 18, 22*); thus, it is conceivable that constitutive expression of *BCL-6*, caused by chromosomal rearrangements, interferes with normal B cell differentiation, thereby contributing to the abnormal lymph node architecture typifying DLCL.

Given that DLCL accounts for ~80% of NHL mortality (*4*), the identification of a specific pathogenetic lesion has important clinicopathologic implications. Lesions in *BCL-6* may help in identifying prognostically distinct subgroups of DLCL. In addition, because a therapeutic response can now be obtained in a substantial fraction of cases (*4*), a genetic marker specific for the malignant clone may be a critical tool for the monitoring of minimal residual disease and early diagnosis of relapse (*29*).

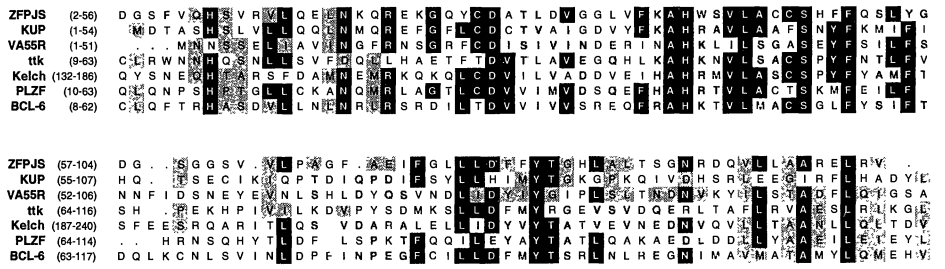

Fig. 2. Homology of the NH_2-terminal region of *BCL-6* to other Krüppel zinc finger proteins, viral (VA55R) proteins, and cellular non–zinc finger (kelch) proteins. Black background indicates identical residues found four or more times at a given position, and gray indicates conserved residues that appear in at least four sequences at a given position. Conserved amino acid substitutions are defined according to the scheme (P, A, G, S, T), (Q, N, E, D), (H, K, R), (L, I, V, M), and (F, Y, W) (*30*). Numbering is with respect to the methionine initiation codon of each gene.

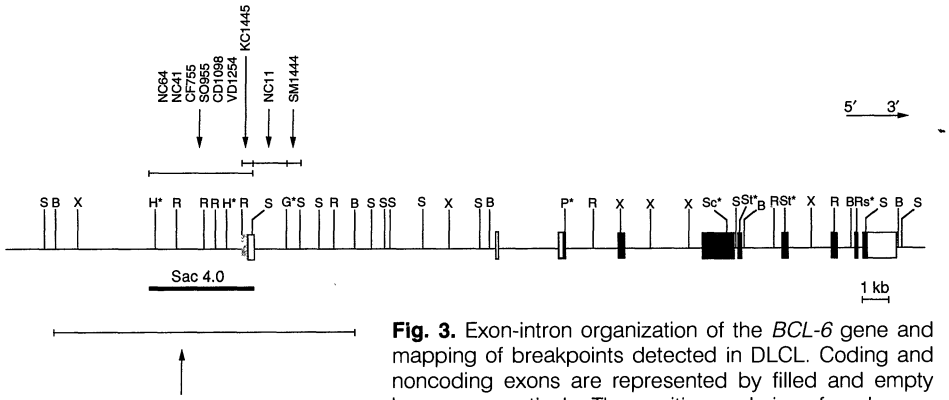

Fig. 3. Exon-intron organization of the *BCL-6* gene and mapping of breakpoints detected in DLCL. Coding and noncoding exons are represented by filled and empty boxes, respectively. The position and size of each exon are approximate and have been determined by the pattern of hybridization of various cDNA probes as well as by the presence of shared restriction sites in the genomic and cDNA. The putative first, second, and third exons have been sequenced in the portions overlapping the cloned cDNA sequences. The transcription initiation site has not been mapped (shaded box on 5′ side of first exon). Patient codes (such as NC11 and 891546) are grouped according to the rearranged patterns displayed by tumor samples. Arrows indicate the breakpoint position for each sample as determined by restriction enzyme–hybridization analysis. For samples KC1445 and SM1444, the breakpoints have been cloned and the precise positions are known. Restriction sites marked by asterisks have been only partially mapped within the *BCL-6* locus. Restriction enzyme symbols are S, Sac I; B, Bam HI; X, Xba I; H, Hind III, R, Eco RI; G, Bgl II; P, Pst I; Sc, Sca I; and St, Stu I. Tumor samples were collected and analyzed for histopathology at Memorial Sloan-Kettering Cancer Center or at Columbia University.

REFERENCES AND NOTES

1. R. S. K. Chaganti *et al.*, in *Molecular Diagnostics of Human Cancer*, M. Furth and M. Greaves, Eds. (Cold Spring Harbor Laboratory, Cold Spring Harbor, NY, 1989), pp. 33–36.
2. B. N. Nathwani, in *Neoplastic Hemopathology*, D. M. Knowles, Ed. (Williams & Wilkins, Baltimore, MD, 1992), pp. 555–601.
3. Y. Tsujimoto, J. Cossman, E. Jaffe, C. M. Croce, *Science* **228**, 1440 (1985); M. L. Cleary and J. Sklar, *Proc. Natl. Acad. Sci. U.S.A.* **82**, 7439 (1985); A. Bakshi *et al.*, *Cell* **41**, 899 (1985); reviewed by S. J. Korsmeyer, *Blood* **80**, 879 (1992).
4. I. T. Magrath, in *The Non-Hodgkin's Lymphomas*, I. T. Magrath, Ed. (Arnold, London, 1990), pp. 1–14.
5. R. Dalla-Favera *et al.*, *Proc. Natl. Acad. Sci. U.S.A.* **79**, 7824 (1982); R. Taub *et al.*, *ibid.*, p. 7837; reviewed by R. Dalla-Favera, in *Causes and Consequences of Chromosomal Translocations*, I. Kirsch, Ed. (CRC Press, Boca Raton, FL, 1993), pp. 313–321.
6. Y. Tsujimoto *et al.*, *Nature* **315**, 340 (1985); T. C. Meeker *et al.*, *Blood* **74**, 1801 (1989); T. Motokura *et al.*, *Nature* **350**, 512 (1991); M. E. Williams, T. C. Meeker, S. H. Swerdlow, *Blood* **78**, 493 (1991); M. Raffeld and E. Jaffe, *ibid.*, p. 259.
7. M. Ladanyi, K. Offit, S. J. Jhanwar, D. A. Filippa, R. S. K. Chaganti, *Blood* **77**, 1057 (1991).
8. K. Offit *et al.*, *Br. J. Haematol.* **72**, 178 (1989).
9. K. Offit *et al.*, *Blood* **74**, 1876 (1989); C. Bastard *et al.*, *ibid.* **79**, 2527 (1992); R. S. K. Chaganti, unpublished data.
10. B. H. Ye, P. H. Rao, R. S. K. Chaganti, R. Dalla-Favera, *Cancer Res.* **53**, 2732 (1993); B. W. Baron *et al.*, *Proc. Natl. Acad. Sci. U.S.A.* **90**, 5262 (1993).
11. A phage cDNA library constructed from RNA of the Bjab lymphoma cell line was screened (1 × 10^6 plaques) by plaque hybridization with the Sac 4.0 probe that had been ^{32}P-labeled by random priming [A. P. Feinberg and B. Vogelstein, *Anal. Biochem.* **132**, 6 (1983)]. The longest insert of the four phages isolated was subcloned into the pGEM-7Zf(−) plasmid (Promega) and sequenced on both strands.

12. M. Kozak, *J. Cell. Biol.* **108**, 229 (1989).
13. Sequences were analyzed with the Genetics Computer Group (GCG) programs on a mainframe computer. Sequence homology searches were carried out through the BLAST E-mail server at the National Center for Biotechnology Information, National Library of Medicine, Bethesda, MD.
14. T. El-Baradi and T. Pieler, *Mech. Dev.* **35**, 155 (1991).
15. J.-P. Kerckaert *et al.*, *Nat. Genet.* **5**, 66 (1993).
16. U. B. Rosenberg *et al.*, *Nature* **319**, 336 (1986); E. J. Bellefroid *et al.*, *DNA* **8**, 377 (1989).
17. W. Knochel *et al.*, *Proc. Natl. Acad. Sci. U.S.A.* **86**, 6097 (1989).
18. E. J. Bellefroid, D. A. Poncelet, P. J. Lecocq, O. Revelant, J. A. Martial, *ibid.* **88**, 3608 (1991).
19. M. M. Sugawara *et al.*, listed as unpublished sequence in NewGenBank (29 May 1993).
20. S. D. Harrison and A. A. Travers, *EMBO J.* **9**, 207 (1990); P. R. DiBello, D. A. Withers, C. A. Bayer, J. W. Fristrom, G. M. Guild, *Genetics* **129**, 385 (1991).
21. P. Chardin, G. Courtois, M.-G. Mattei, S. Gisselbrecht, *Nucleic Acid Res.* **19**, 1431 (1991).
22. Z. Chen *et al.*, *EMBO J.* **12**, 1161 (1993).
23. E. V. Koonin, T. G. Senkevich, V. I. Chernos, *Trends Biochem. Sci.* **17**, 213 (1992).
24. F. Xue and L. Cooley, *Cell* **72**, 681 (1993).
25. B. H. Ye *et al.*, unpublished data.
26. A phage genomic library constructed from normal human placenta DNA (Stratagene) was screened (8×10^5 plaques) with the *BCL-6* cDNA (*11*). Twelve overlapping clones spanning ~50 kb of genomic DNA were isolated. After restriction mapping, the position of various *BCL-6* exons was determined by Southern hybridization with various cDNA probes.
27. A *BCL-6* transcript of normal size was detected by Northern blot analysis of DLCL cells carrying either normal or truncated *BCL-6*. Some of the truncations were in the 5′ flanking sequences and would therefore not be expected to generate structurally abnormal transcripts.
28. *PML*, H. de Thé *et al.*, *Cell* **66**, 675 (1991); A. Kazizuka *et al.*, *ibid.*, p. 663; P. P. Pandolfi *et al.*, *Oncogene* **6**, 1285 (1991); *EVI-1*, K. Morishita *et al.*, *Cell* **54**, 831 (1988); S. Fichelson *et al.*, *Leukemia* **6**, 93 (1992); *TTG-1*, E. A. McGuire *et al.*, *Mol. Cell. Biol.* **9**, 2124 (1989); *HTRX*, M. Djabali *et al.*, *Nat. Genet.* **2**, 113 (1992); D. C. Tkachuk, S. Kohler, M. L. Cleary, *Cell* **71**, 691 (1992); Y. Gu *et al.*, *ibid.*, p. 701; *WT-1*, D. A. Haber *et al.*, *ibid.* **61**, 1257 (1990).
29. L. J. Medeiros *et al.*, in (*2*), pp. 263–298.
30. Abbreviations for the amino acid residues are A, Ala; C, Cys; D, Asp; E, Glu; F, Phe; G, Gly; H, His; I, Ile; K, Lys; L, Leu; M, Met; N, Asn; P, Pro; Q, Gln; R, Arg; S, Ser; T, Thr; V, Val; W, Trp; and Y, Tyr.
31. We thank Y. Zhang, S. Shammah, C.-C. Chang, G. Gaidano, and T. Saksela for reagents and advice. Supported by NIH grants CA 44029 (R.D.-F.), CA 48236 and EY 06337 (D.M.K.), and CA 34775 and CA 08748 (R.S.K.C.). F.L.C. is supported in part by Associazione Italiana contro le Leucemie (AIL).

9 July 1993; accepted 31 August 1993

Isolation of the Cyclosporin-Sensitive T Cell Transcription Factor NFATp

Patricia G. McCaffrey, Chun Luo, Tom K. Kerppola, Jugnu Jain, Tina M. Badalian, Andrew M. Ho, Emmanuel Burgeon, William S. Lane, John N. Lambert, Tom Curran, Gregory L. Verdine, Anjana Rao,* Patrick G. Hogan

Nuclear factor of activated T cells (NFAT) is a transcription factor that regulates expression of the cytokine interleukin-2 (IL-2) in activated T cells. The DNA-binding specificity of NFAT is conferred by NFATp, a phosphoprotein that is a target for the immunosuppressive compounds cyclosporin A and FK506. Here, the purification of NFATp from murine T cells and the isolation of a complementary DNA clone encoding NFATp are reported. A truncated form of NFATp, expressed as a recombinant protein in bacteria, binds specifically to the NFAT site of the murine IL-2 promoter and forms a transcriptionally active complex with recombinant c-Fos and c-Jun. Antisera to tryptic peptides of the purified protein or to the recombinant protein fragment react with T cell NFATp. The molecular cloning of NFATp should allow detailed analysis of a T cell transcription factor that is central to initiation of the immune response.

Nuclear factor of activated T cells is an inducible DNA-binding protein that binds to two independent sites in the IL-2 promoter (*1*, *2*). NFAT is a multisubunit transcription factor (*3*) consisting of at least three DNA-binding polypeptides, the preexisting subunit NFATp (*4–6*) and homodimers or heterodimers of Fos and Jun family proteins (*6–9*). NFATp is present in the cytosolic fraction of unstimulated T cells (*3–7*); after T cell activation, it is found in nuclear extracts and forms DNA-protein complexes with Fos and Jun family members at the NFAT sites of the IL-2 promoter (*3*, *5–9*). NFATp has also been implicated in the transcriptional regulation of other cytokine genes, including the genes for granulocyte-macrophage colony-stimulating factor (GM-CSF), IL-3, IL-4, and tumor necrosis factor–α (TNF-α) (*10*).

NFATp is the target of a Ca^{2+}-dependent signaling pathway initiated at the T cell receptor (*3*, *4*, *6*, *7*, *11–13*). The rise in intracellular free Ca^{2+} in activated T cells results in an increase in the phosphatase activity of the Ca^{2+}- and calmodulin-dependent phosphatase calcineurin (*14*). NFATp is a substrate for calcineurin in vitro (*4*, *6*) and is thought to be dephosphorylated by calcineurin in activated T cells, resulting in its translocation from the cytoplasm to the nucleus (*13*). Cyclosporin A (CsA) and FK506, which act as a complex with their respective intracellular receptors to inhibit the phosphatase activity of calcineurin (*15*), block the dephosphorylation of NFATp (*4*) and the appearance of NFAT in nuclear extracts of stimulated T cells (*2*, *3*, *7*, *12*). This mechanism may account for the sensitivity to cyclosporin of IL-2 and other cytokine genes (*10*, *13*) and thus for the profound immunosuppression caused by CsA and FK506 (*13*).

NFATp was purified from the C1.7W2 cell line (*16*), a derivative of the murine T cell clone Ar-5 (*17*), by ammonium sulfate fractionation followed by successive chromatography on a heparin-agarose column and an NFAT oligonucleotide affinity column (*18*). A silver-stained SDS gel of the purified protein showed a major broad band migrating with an apparent molecular size of ~120 kD (Fig. 1, top). We have shown that this band contains a DNA-binding phosphoprotein that is dephosphorylated by calcineurin to yield four sharp bands migrating with apparent molecular sizes of ~110 to 115 kD (*6*). NFATp DNA-binding activity was demonstrable in protein eluted from the SDS gel and renatured (*4*), and more than 90% of the activity recovered from the gel comigrated with the ~120-kD band (Fig. 1, lane 7). The faster migrating complexes formed with proteins of slightly smaller molecular size (lanes 8 to 11) most likely derive from partial proteolysis. The purified protein binds to the NFAT site with the appropriate specificity and forms a DNA-protein complex with recombinant Fos and Jun (*6*).

To confirm that the 120-kD protein was the preexisting subunit of the T cell transcription factor NFAT, we used antisera to tryptic peptides derived from the 120-kD protein (*18*). When one such antiserum (to peptide 72) was included in the binding reaction, it "supershifted" the NFATp-DNA complex formed by the cytosolic fraction from unstimulated T cells (Fig. 2, lane

P. G. McCaffrey, C. Luo, J. Jain, T. M. Badalian, E. Burgeon, A. Rao, Division of Tumor Virology, Dana-Farber Cancer Institute, and Department of Pathology, Harvard Medical School, Boston, MA 02115.
T. K. Kerppola and T. Curran, Department of Molecular Oncology and Virology, Roche Institute of Molecular Biology, Roche Research Center, Nutley, NJ 07110.
A. M. Ho and P. G. Hogan, Department of Neurobiology, Harvard Medical School, Boston, MA 02115.
W. S. Lane, Microchemistry Facility, Harvard University, Cambridge, MA 02138.
J. N. Lambert and G. L. Verdine, Department of Chemistry, Harvard University, Cambridge, MA 02138.
*To whom correspondence should be addressed.